Not to be cited without
permission of the authors[1]

Canadian Atlantic Fisheries
Scientific Advisory Committee

CAFSAC Research Document 91/79

Ne pas citer sans
autorisation des auteurs[1]

Comité scientifique consultatif des pêches
canadiennes dans l'Atlantique

CSCPCA Document de recherche 91/79

THE NORTHERN SHRIMP BIOMASS IN THE SEPT-ILES REGION OF THE GULF OF ST.LAWRENCE DURING THE 1980'S: A GEOSTATISTICAL ESTIMATION

by

YVAN SIMARD

Institut Maurice-Lamontagne, Ministère des Pêches et des Océans,
C.P. 1000, Mont-Joli, Québec G5H 3Z4

---

[1] This series documents the scientific basis for fisheries management advice in Atlantic Canada. As such, it addresses the issues of the day in the time frames required and the Research Documents it contains are not intended as definitive statements on the subjects addressed but rather as progress reports on ongoing investigations.

Research Documents are produced in the official language in which they are provided to the Secretariat by the author.

[1] Cette série documente les bases scientifiques des conseils de gestion des pêches sur la côte atlantique du Canada. Comme telle, elle couvre les problèmes actuels selon les échéanciers voulus et les Documents de recherche qu'elle contient ne doivent pas être considérés comme des énoncés finals sur les sujets traités mais plutôt comme des rapports d'étape sur les études en cours.

Les Documents de recherche sont publiés dans la langue officielle utilisée par les auteurs dans le manuscrit envoyé au secrétariat.

RESUME

Des méthodes de la géostatistique stationnaire sont employées pour produire des estimés globaux et partiels de la biomasse de crevette nordique (Pandalus borealis) présente dans la région de Sept-Iles à l'automne des années 1982, 1984, 1985, 1987 à 1990. Les échantillons de biomasse ont été récoltés pendant le jour à partir de chalutiers équipés de chaluts à crevette. Des modèles isotropiques de la variabilité spatiale sont estimés à partir des données, séparément pour chaque année, et ensuite utilisés pour calculer les estimés et leur intervalle de confiance. Le modèle spatial ainsi que les paramètres de krigeage optimaux sont choisis d'après les résultats de tests de validation de type "jackknife". Les estimés sont calculés pour deux enveloppes séparément, l'une à l'est, l'autre à l'ouest. Les résultats de krigeage sont comparés aux estimés calculés par tessellation polygonale.

Les estimés globaux montrent que la biomasse dans l'aire d'étude est passée de 4.8 à 10.4 kt pendant la période d'observation. Les estimés partiels indiquent que la biomasse contenue dans les zones plus riches que 1 t/km^2 a changé par un facteur 10 pendant cette période, passant de 0.9 à 9.5 kt. Le bassin de la Grande Coulée, à l'est, est responsable de la plus grande part de l'accroissement de la biomasse.

ABSTRACT

Stationary geostatistical methods are used to compute global and partial estimates of the biomass of northern shrimp (Pandalus borealis) present in the Sept-Iles region in the falls of 1982, 1984, 1985, and 1987 to 1990. Biomass samples were collected during daylight from trawlers equipped with shrimp bottom trawls. Isotropic models of the spatial variability are estimated from the data, for each year separately, and are used for estimating the biomass and its confidence interval. The optimal model and kriging parameters for the estimation are chosen from the results of "jackknife" cross-validation tests. The estimates are computed separately for two envelopes, one on the east of the region, the other on the west. Kriging results are compared to an alternative estimation from polygonal tessellation.

Global estimates showed that the biomass in the area under study increased from 4.8 to 10.4 kt during the period of observation. Partial estimates indicated that the biomass of the areas richer than 1 t/km^2 changed by one order of magnitude, from 0.9 to 9.5 kt during the same period. The eastern basin was responsible for the major part of the biomass increase.

INTRODUCTION

The northern shrimp biomass in the western Gulf of St.Lawrence (Fig 1.) is not randomly or regularly distributed through space but present well-defined structures, characterized by gradients, recurrent patches or holes, and other complex patterns. In such case, the biomass at one location is correlated with the biomass at nearby locations. This spatial autocorrelation requires special considerations in estimating the standing stocks of shrimp (Simard et al. 1992). In classical statistics, when the spatial structure is known and stable through time, the space is often discretized into homogeneous strata, where spatial structuring is assumed to be absent or negligeable. Independent allocation of the samples may then be optimised by a stratified plan, in order to minimize the variance of the estimate and the structure-dependent bias. When the spatial structure is unknown or unstable through time, as it is the rule for the northern shrimp in the Gulf of St.Lawrence (Simard 1989, unpublished MS), stratified sampling is ineffective.

Geostatistics is an alternative to the classical statistics framework for dealing with spatially autocorrelated phenomena. It makes use of the additional information provided by autocorrelation for computing estimates and their confidence intervals. Its application to the estimation of exploited marine resources have been explored recently (Conan 1985, Nicolajsen and Conan 1987, Armstrong et al. 1989, Petitgas and Poulard 1989), with variable success. The present study uses stationary geostatistical methods to estimate the fall biomass of the northern shrimp in the Sept-Iles region of the western Gulf of St.Lawrence (Fig. 1) during the last decade. Two types of estimates are computed: **global estimates** of the total biomass in the study area, defined by the east and west envelopes of Fig. 1, and **partial estimates**, which delineate the area where the biomass exceeds given threshold values and the biomass it incorporates. These later estimates define the exploitable tonnage and the richest areas, expected to be the most profitable. The kriging global estimates computed are compared to the corresponding estimates obtained from polygonal tessellation, which consists of weighing the samples by their area of influence.

METHODS

Sampling

From August to October 1982-1990, except 1983 and 1986, northern shrimp biomass was sampled at 30-98 stations in the western Gulf of St.Lawrence (Fig. 2, Table 1). At each station, bottom shrimp trawls were towed for 30 minutes at 2.5 - 3.0 knots by chartered shrimp trawlers or the research trawler M/V Alfred Needler (Table 1). The stretched mesh aperture of the trawls was 38 mm and the codend was lined with a 19 mm mesh net. All sampling was carried out during daytime because of possible vertical migrations of the shrimp off the bottom at night (Barr 1970, Apollonio et al. 1986), that could change their capturability. No attempt was made to weigh all the catches by a capturability coefficient, to take into account the sampling efficiency of the trawls and the shrimp availability to the fishing gear. However the Alfred Needler catches in 1989 were converted to Bradelle catches by means of a linear regression computed from paired samples ($r^2 = 0.82$). The catches were converted to biomass of northern shrimp per bottom surface unit (kg/km^2). Although the samples were not punctual but covered an average area of 14.5 m by about 2.5 km ($\approx$ 0.035 km^2), they were considered as point samples centered at the starting tow coordinates for further analysis.

Geostatistical estimation

From the geostatistical theory (Matheron 1971), we postulate that the actual biomass of shrimp at one location and one moment is the result of the realization of an underlying probabilistic spatial model. When the characteristics of this model are known, it is possible to estimate the value of the biomass at any point in space.

For the present estimations, we first started by estimating and validating the spatial model from the samples for each year, assuming stationary conditions (below). Then, the models were used to interpolate point estimates at the nodes of a regular grid, bounded by the contour of the estimation areas, according to ordinary point kriging (Journel and Huijbregts 1978, Clark 1979, Isaaks and Srivastava 1989). The point estimates were averaged, and these means were weighted by the surface of the estimation envelopes to obtain the global estimates. Partial estimates of the biomass surpassing the cutoffs of 0.5, 1.0 and 1.5 t/km^2, were obtained similarly, using only the point estimates exceeding the cutoffs. Finally, the variances of these estimates were computed using the estimated spatial model, according to the combination of the average elementary sampling error (Journel and Huijbregts 1978, chap. V.C.2; see Simard et al. 1992).

Variogram. The spatial model is described by the variogram (strictly, the semi-variogram), **gamma(h)**, a function which expresses how the difference in biomass between two locations is related to their geographic distance separation **(h)**:

$$\mathrm{VAR}[Z(x+h)-Z(x)] = 2\,\mathrm{gamma}(h) \tag{1}$$

$$E[Z(x+h)-Z(x)] = 0 \tag{2}$$

For each year these variograms were estimated from the samples assuming the second order weak stationarity conditions described by equations (1) and (2) (known as the intrinsic hypothesis). All the mixed model used (Table 2, Fig. 3) incorporated: 1) a term, the constant C_0 (= **nugget parameter**), representing the sampling error and the unresolved small-scale variability, and 2) a spatial structure, described by either a **linear model** (**gamma(h) = bh**) or a **spherical model** (**gamma(h) = C_1 [$3h/2a - h^3/2a^3$]** if **h** ≤ **a** and **(h)** = **C_1** if **h > a**, where **a** is the range of autocorrelation and C_1 is the plateau of semi-variance or the sill). Because significant anisotropy could not be clearly evidenced from the small sets of samples collected, all variograms computed were omnidirectional. The performance of the variogram models fitted and of the possible kriging parameters was examined by a cross-validation procedure (see below).

Local Estimation. Local estimation[1] of the biomass $Z^*(x_0)$ at a point x_0 was done by interpolation using the data points $Z(x_i)$ available in the surrounding neighborhood chosen:

$$Z^*(x_0) = \sum_{i=1}^{n} w_i \bullet Z(x_i) \tag{3}$$

where the w_i are weights. They sum to 1 to insure that the estimate is unbiased. The w_i are estimated in such a way that they minimize the variance of the error of the estimate, called the kriging variance ($\sigma_k^{*2}(x_0) = \mathrm{VAR}[Z^*(x_0) - Z(x_0)] =$ **minimum**). The solution to minimize $\sigma_k^{*2}(x_0)$ is obtained by partial differentiation relative to the weights w_i, taking into account that they must sum to 1 (for details see Isaaks and Srivastava 1989).

---

[1] The superscript star distinguishes estimates from true values.

The matrix equation system to solve is:

$$C \qquad \bullet \qquad W \qquad = \qquad U \qquad\qquad (4)$$

$$\begin{bmatrix} C^*_{11} & \cdots & C^*_{1n} & 1 \\ \vdots & \ddots & \vdots & \vdots \\ C^*_{n1} & \cdots & C^*_{nn} & 1 \\ 1 & \cdots & 1 & 0 \end{bmatrix} \bullet \begin{bmatrix} w_i \\ \vdots \\ w_n \\ \mu \end{bmatrix} = \begin{bmatrix} C^*_{10} \\ \vdots \\ C^*_{n0} \\ 1 \end{bmatrix}$$

where the C^*_{ij} are the covariances between the shrimp biomass corresponding to the samples ($C^*_{ij} = E\{ [Z(x_i) - E(Z(x_i))] \bullet [Z(x_j) - E(Z(x_j))]\}$) that describe the spatial structure of the probabilistic model. The Lagrange parameter μ is a mathematical artifice introduced to constrain the weights to sum to 1. The C^*_{ij} are calculated by means of the function $C^*(h) = \mathbf{gamma}^*(\infty) - \mathbf{gamma}^*(h)$, where $\mathbf{gamma}^*(h)$ is the estimated variogram and $\mathbf{gamma}^*(\infty)$ is its sill. This sill is equal to the variance of the population (σ^2) under stationarity conditions, when the sampled field is larger than the spatial structure. Since $\mathbf{gamma}^*(\infty)$ is a constant, the covariance terms, C^*, in equation (4) are replaced by the variograms $\mathbf{gamma}^*$ without changing the equality. Then the weights are found by solving $W = C^{-1} \bullet U$, and they are substituted in equation (3) to get the biomass estimate $Z^*(x_0)$ looked for. The corresponding minimized error variance of this estimate, $\sigma_k^{*2}(x_0)$, is obtained from the following matrix equation:

$$\sigma_k^{*2}(x_0) \quad = \quad \sigma^{*2} - W \bullet U \qquad\qquad (5)$$

where σ^{*2} is the variance of the samples.

In practice, local estimates are computed using only the most significant samples included in a confined ellipse-shaped neighborhood moving throughout the sampled region. The definition of this neighborhood, the chosen maximum number of data points to consider and their search method (nearest points in each octant or quadrant, or in the whole ellipse) affect the value of the local estimates (see guidelines in Isaaks and Srivastava 1989). Since there are always many possible choices for all the above factors that affect the kriging estimates and for the variogram model, an optimal set of choices was looked for by cross-validation using a jackknife-type method. In this procedure, the samples were removed one by one and they were estimated using the chosen variogram model, search ellipse and search method. The best solution retained was the one which, among other properties, minimized the mean square residuals, produced the standardized residuals ($[Z^*(x_i) - Z(x_i)] / \sigma_k^{*2}(x_i)$) the closest to the conditional expectations of a mean of 0 and a standard deviation (SD) of 1.0, and maximized the correlation coefficient between the observed and the estimated values, whose linear regression should have a slope close to 1.0 (see Samper Calvete and Neuman 1989). Finally for computing the point estimates, the ellipses were not limited to the envelope of estimation but to the whole region, in order to make maximum use of the information available from the samples set.

Global and partial estimations. Global estimation of the mean biomass density (Z^*) was easily obtained by averaging the **m** local estimates, separately for each envelope to be estimated. The total mass of shrimp ($\mathbf{ZD}^*$) per envelope **D** was then estimated from the equation:

$$ZD^* = S_D \bullet \frac{1}{m} \bullet \sum_{j=1}^{m} Z^*(x_j) \qquad (6)$$

where S_D is the area of the envelope. Partial estimates were obtained similarly, using only the local estimates exceeding the chosen cutoff biomass.

The variance of these estimations can be computed in various ways, depending on the postulates and on the measure of uncertainty looked for (Journel and Huijbregts 1978, Isaaks and Srivastava 1989). Here, we used the combination of the elementary sampling errors of the extension variance approach, as in Simard et al. (1992). The range of reliability of the computed experimental variograms did not allow the use of the usual method for computing the variance per large strata or for the whole envelope in one step (e.g. Petitgas and Poulard 1989). The procedure used computes the variance, σ_D^2, of **ZD** from the formula:

$$\sigma_D^{2*} = \text{mean-gamma}(s,s) \bullet s^2 \bullet N \qquad (7)$$

where **mean-gamma(s,s)** is the average semi-variance within the average elementary sampling unit **s** of surface $\mathbf{s}^2$, **N** is the number of samples in the envelope to be estimated. The dimensions of **s** must respect the length/width ratio of the envelope **D**. This is an easy approximation of σ_D^{2*}, when the sampling density is uniform, which is almost the case here. Its solution can be obtained rapidly from geostatistical charts.

The variance of partial estimations is obtained similarly, except that the variogram used is the one computed using only the samples where the shrimp density exceeds the given cutoff (Froideveaux 1984). Then the unit surface s_c is obtained by dividing the surface of the envelope **D** by the number N_c of samples exceeding the cutoff **c**. When these N_c samples are concentrated in only a fraction of the envelope, the surface of this fraction could be used instead of the surface of the whole envelope.

The estimation of the mean biomass of both envelopes combined ZT^* was obtained by summing the computed mean biomass of the envelopes, weighted by their respective surface S_{Di} as follows:

$$ZT^* = \frac{1}{S_{DT}} \bullet \sum_{i=1}^{2} S_{Di} \bullet Z^*_{Di} \qquad (8)$$

$$\sigma^{2*}_{DT} = \frac{1}{(S_{DT})^2} \bullet \sum_{i=1}^{2} (S_{Di})^2 \bullet \sigma^2_{Di} \qquad (9)$$

where S_{DT} is the sum of the surface of the two envelopes.

Polygonal tessellation

Computation of estimates for each envelope according to polygonal tessellation was obtained from the following equations.

$$ZP^* = \frac{1}{S_D} \bullet \sum_{j=1}^{N} s_j \, Z(x_j) \qquad (10)$$

$$\sigma^2_{DP}{}^* = \frac{1}{S_D} \bullet \sum_{j=1}^{N} s_j \, (Z(x_j)-ZP^*)^2 \qquad (11)$$

Where ZP^* is the mean, s_j are the surface of the Dirichlet's (= Voronoi) polygon of influence of the samples $Z(x_j)$, S_D is their sum; $\sigma^2_{DP}{}^*$ is the variance. The estimates for both envelopes combined are obtained as presented above in equations (9) and (10) for the kriging estimates.

RESULTS AND DISCUSSION

As usually observed in ecological data sets with low number of samples, the variograms computed were relatively erratic and difficult to model (Fig. 3). This resulted from the low number of samples but also from the non-stationarity of the data in space and time. The variability changed with the local mean biomass, and annually with the global abundance. Despite this fact, spatial structures were discernable every year, none of the variograms indicating a pure random variability (constant semi-variance for all separation distances). The unresolved small-scale variability was also always present, but quite variable in amplitude and in its relative contribution to the total variability. In general the variograms exhibited higher similarities at small time lags (a few years), indicating a tendency to a short-term temporal stability. This may however depend on the mean abundance, which is also more similar at small time lags (Table 3). In modeling the variograms, the emphasis was put on the small distances, on which the estimation essentially rely, and the large structures were sometimes neglected.

The high variability of the variograms resulted in a low performance in the cross-validation test, as indicated from the low correlations of the observed vs the predicted values of the samples (Table 2). The slopes of the corresponding linear regressions were smaller than 1, indicating that, on average, the spatial models underestimated the low values and overestimated the high values, a common feature of kriging ("conditional bias": Isaaks and Srivastava 1989). The SD of errors of the estimates indicated however that the performance of kriging was always much better than the alternative polygonal tessellation. The estimation was often very sensitive to the size of the neighborhood and to the number of points used for kriging. The optimal solutions obtained (Table 2, underlined) changed from year to year from a small neighborhood including only 2 points, to a neighborhood of a radius of 50 km including as many as 12 points.

Estimation

The kriging estimates of the global biomass of northern shrimp in the study area indicated that the biomass varied from 5 kt to 10 kt during the study period (Table 3). The major part of the biomass was always located in the largest west envelope, but the east envelope contribution reached almost 50% of the total biomass in 1988 and 1989 (Fig. 4). The relative errors on these estimates were low (7-13%) for the total biomass and for the west envelope, but quite variable (6-31%) for the biomass of the east envelope (Table 3). Since this latter envelope represented the smallest fraction of the total biomass, the **absolute** error on its biomass was generally comparable or smaller than the absolute error on the west envelope biomass (Fig.4). Therefore the occasional large relative error of the east stratum did not strongly affect the estimates of the total biomass (Table 3, Fig. 4).

Except for the confidence intervals (when computable), the partial estimates of the tonnage corresponding to the areas where the biomass density exceeds 0.5, 1.0 and 1.5 t/km^2 exhibited notable different patterns compared to the global estimates (Table 3, Fig 5). First, their interannual fluctuations in each envelope and in the whole region were more pronounced. The total tonnage profitably exploitable (biomass density > 1.0 t/km^2) increased more rapidly than the global tonnage (Figs. 4 and 5). It showed extremely low values in 1984 despite the fact that the total biomass remained constant. From the surface increase of these dense areas (Table 3), the shrimps did not concentrate more intensively in some years. The densest areas rather spreaded and shrinked, with their center of mass moving from year to year (Fig. 2). The proportion of the profitably exploitable total tonnage peaked to 92% in 1990, while the mean biomass was two folds higher than the lowest value of 1984. Clearly, the saturation of the habitat increased, especially in the east envelope where the average biomass density peaked in 1989 to 2.7 t/km^2. Our knowledge of the ecology of the northern shrimp is presently too poor to say if the present maximum density is close to the support capacity of the habitat. The east envelope is however closer to this limit than the west envelope.

The estimation of the global biomass from the alternative methods of the polygonal tessellation or the arithmetic mean were generally close to the kriging estimates (Table 3). The relatively uniform distribution of the samples in space is responsible for this good performance, by allowing the measurement of the spatial variation over the whole envelopes. This would not have been the case if the samples had been clustered in limited zones of the study area. The relative performance of polygonal tessellation was however better than the arithmetic mean, the ratio of its estimate vs the kriging estimate being generally closer to the value of 1.0 (Fig. 6). This was due to the sample-declustering property of this method (Isaaks and Srivastava 1989), which allows it to properly weigh the samples relative to their importance to the global estimate. This is not done with the arithmetic mean, where all the samples have the equal weight of 1/N. The optimal weights are obtained from kriging, which has been called for this reason the Best Linear Unbiased Estimator (BLUE). Because kriging is an

interpolation method, known as optimal, in presence of spatial structures, its mean estimates will always be better than the alternative methods, even though the structures are poorly modeled, because it will always appropriately weight the data and take the structure (by interpolating) into account. It is therefore recommended for estimating the shrimp biomass, because this biomass is clearly spatially structured and this spatial structure is not yet predictable. It is also recommended to maintain or even enhance the quasi uniform distribution of the samples in the survey areas, to keep the quality of the spatial information of the data set.

CONCLUSION

In conclusion, the present exploitation of geostatistics to estimate the biomass of northern shrimp in the western Gulf of St.Lawrence has clearly evidenced a strong increase of the global biomass in the last decade. This increase is much more related to the increase in biomass in the Grande Coulée basin, circled by the east envelope, than to the rest of the surveyed region. This basin made significant contributions since 1988, and its high biomass density, which peaked in 1989, now seems to overflow in the west basin. This latter observation is in accordance with the local ontogenic migration routes postulated by Simard and Savard (1990).

Despite the large variability of the biomass, there are some phenomena that show more stability and which need more attention. First, the variograms are temporally autocorrelated. This points out a degree of temporal stability which could be taken into account to enhance the reliability of the geostatistical spatial model. It also reveals that the changes in the total biomass are smoothed over a few years and they last for more than one year. This temporal consistency also stresses that the fluctuations in the global estimates cannot be attributed to temporal bias related to the efficiency of sampling. Second, there seems also to be a spatially ordered displacement of the rich patches from year to year. Confirmation of this however will need a more detailed geostatistical study of the spatial organization. Finally, the reasons for the present large increase of biomass in the Grande Coulée basin must be meticulously investigated, because of their strong importance to explain the fluctuations of the total biomass. For this reason, it is important to maintain the annual dense shrimp sampling program in the western Gulf of St.Lawrence in order to be able to monitor and study the significant phenomenon that is presently occurring in the local shrimp population.

ACKNOWLEDGMENT

I am grateful to Louise Savard, Philippe Jalbert, Sylvain Hurtubise, and other colleagues who contributed to different steps of the study. I am especially indebted to our late colleague Estelle Laberge for her large contribution to the 1990 sampling program. Kriging estimates were computed using GEO-EAS (EPA, USA) and other geostatistics software used at the Ecole Polytechnique de Montréal (Montréal, Québec).

REFERENCES

Armstrong, M., D. Renard and P. Berthou. 1989. Applying geostatistics to the estimation of a population of bivalves. ICES C.M.1989/K37, 22 p.

Apollonio, S., D.K. Stevenson, and E.E. Dunton. 1986. Effects of temperature on the biology of the northern shrimp, Pandalus borealis, in the Gulf of Maine. U.S. Dept. of Commerce, NOAA Tech. Rep. NMFS no. 42, 22 p.

Barr, L. 1970. Diel vertical migration of Pandalus borealis in Kachemak bay, Alaska. J. Fish. Res. Board Can. 27: 669-676.

Clark, I. 1979. Practical geostatistics. Elsevier, N.Y.

Cliff, A.D., and J.K. Ord. 1981. Spatial processes: models and applications. Pion Ltd., London, U.K. 266 p.

Conan, G. 1985. Assessment of shellfish stocks by geostatistical techniques. NAFO SCR Doc. 85/108, 19p.

Froideveaux, R. 1984. Precision of estimation of recoverable reserves: The notion of conditional estimation variance. p. 141-164. In. Verly, G. et al. (eds.) Geostatistics for natural resources characterization. NATO ASI Series C, Vol. 122. Reidel, Dordrecth.

Isaaks, E.H., and R. M. Srivastava. 1989. Applied geostatistics. Oxford University Press, N.Y. 561 p.

Journel, A.G.,and Ch. J. Huijbregts. 1978. Mining geostatistics. Academic Press, N.Y. 600 p.

Nicolajsen, A., and G. Conan. 1987. Assessment by geostatistical techniques of populations of Iceland Scallop (Chlamis islandica) in the Barent sea. I.C.E.S. CM 1987/K:14, 18 p.

Petitgas, P., and J.-C. Poulard. 1989. Applying stationary geostatistics to fisheries: a study on hake in the bay of Biscay. ICES, Demersal Fish. Committee. C.M./G.62. 21 p.

Samper Calvete, F.J., and S.P. Neuman. 1989. Geostatistical analysis of groundwater quality data from the Madrid basin using adjoint state maximum likelihood cross-validation. p. 725-736. In M. Armstrong (ed.). Geostatistics, Vol. 2. Kluwer Academic Publishers, The Netherlands.

Savard, L. 1989. Evaluation des stocks de crevette (Pandalus borealis) du Golfe du Saint-Laurent. Comité Sci. Consul. Pêches Can. Atlant. (CSCPCA), Doc. Rech. 89/07, 70p.

Simard, Y. 1989, unpublished MS. Changes in spatial patterns of biomass and exploitation intensity of the northern shrimp in the gulf of St.Lawrence as indicated by maps obtained from kriging. I.C.E.S./Workshop on Spatial Statistics, Brest, 16-19 May. Work. pap. 15p.

Simard, Y., P. Brunel and J. Lacelle. 1990. Distribution and growth of pre-recruit cohorts of the northern shrimp (Pandalus borealis) in the western Gulf of St.Lawrence as related to hydrographic conditions. Can. J. Fish. Aquat. Sci. 47: 1526-1533.

Simard, Y., P. Legendre, G. Lavoie et D. Marcotte. 1992. Mapping, estimating biomass, and optimizing sampling programs for spatially autocorrelated data: case study of the northern shrimp (Pandalus borealis). Can. J. Fish. Aquat. Sci. 49: 32-45.

Simard, Y., and L. Savard, 1990. Variability, spatial patterns and scales of similarity in size-frequency distributions of the northern shrimp (Pandalus borealis) and its migrations in the Gulf of St.Lawrence. Can. J. Fish. Aquat. Sci. 47: 794-804.

Table 1. Trawl samples collected in the northwestern Gulf of St.Lawrence during research surveys for estimating the northern shrimp biomass at the end of the summer, and used here for computing the kriging estimates.

YEAR	VESSEL	LENGTH (m)	TRAWL TYPE	NO OF SAMPLES
1982	M/V Vicky & Bros.	27	Yankee 36	30
1984	M/V Marie-Bernard	27	Western IIA	49
1985	M/V Saïda	27	Western IIA	38
1987	M/V G.C. Global	25	Western IIA	53
1988	M/V G. C. Global	25	Western IIA	42
1989	M/V A. Needler	50	URI 81-114	16
	M/V Bradelle	27	Western IIA	82
	Total:			98
1990	M/V A. Needler	50	URI 81-114	18
	M/V Marie-Simon	20	Western IIA	46
	Total:			64

Table 2. Cross-validation of the search parameters for kriging. SD of errors (SD_E) of the estimates from the true value ($Z^*(x_i)-Z(x_i)$) at the sample points (x_i), obtained using the given variogram and the search parameters; Pearson correlation coefficients (r1 and r2) and slopes (b1 and b2) of the linear regressions $\ln (Z+1) = a1 + b1 (\ln Z^*+1)$ and $Z = a2 + b2 Z^*$; mean, SD, and maximum values of standardized residuals ($Z^*(x_i)-Z(x_i) / \sigma_k^*(x_i)$). Underlined are the chosen combinations for kriging.

YEAR	VARIOGRAM	SEARCH RADIUS (km)	MAX. NO POINTS	SD_E	r1	b1	r2	b2	STANDARDIZED RESIDUALS		
									Mean	SD	max
1982	Isotropic, nugget + spherical gamma(h) = 200000 + 400000 $Sph_{85}(h)$	25	8	646	0.56	0.83	0.34	0.62	0.01	1.12	-3.1
		"	4	630	0.59	0.80	0.40	0.67	-0.05	1.08	-3.1
		"	2	703	0.53	0.60	0.42	0.32	0.08	1.14	-3.1
	Polygonal tessellation (estimate = nearest sample)	200	1	850	0.29	0.33	0.05	0.16	--	--	--
1984	Isotropic, nugget + linear gamma(h) = 110000 + 1818 h	50	12	445	0.29	0.97	0.24	0.59	0.03	1.16	-3.3
		25	12	445	0.29	0.97	0.24	0.59	0.03	1.16	-3.3
		25	8	459	0.26	0.80	0.20	0.43	0.08	1.18	-3.2
		"	4	468	0.24	0.70	0.19	0.36	0.16	1.18	-3.6
		"	2	506	0.32	0.44	0.17	0.29	0.02	1.18	-3.8
	Polygonal tessellation (estimate = nearest sample)	200	1	571	0.33	0.37	0.15	0.16	--	--	--
1985	Isotropic, nugget + linear gamma(h) = 220000 + 2600 h	50	12	596	0.10	0.10	0.25	0.41	-0.04	1.01	-2.7
		"	8	534	0.29	0.84	0.38	0.84	0.05	0.98	-2.5
		25	8	592	0.11	0.11	0.27	0.43	-0.03	1.00	-2.7
		"	4	615	0.11	0.11	0.25	0.36	-0.02	1.02	-2.7
		"	2	645	0.09	0.10	0.20	0.27	-0.01	1.01	-2.7
	Isotropic, nugget + spherical gamma(h) = 120000 + 200000 $Sph_{30}(h)$	50	12	536	0.39	1.05	0.38	0.77	0.02	1.05	-2.6
		"	8	528	0.41	1.12	0.41	0.82	0.04	1.02	-2.4
		25	8	589	0.14	0.14	0.30	0.45	-0.05	1.05	-2.6
		"	4	609	0.14	0.14	0.27	0.38	-0.03	1.08	-2.6
		"	2	632	0.12	0.12	0.23	0.31	-0.07	1.07	-2.6
	Polygonal tessellation (estimate = nearest sample)	200	1	609	0.23	0.21	0.31	0.40	--	--	--

Table 2. (cont.)

YEAR	VARIOGRAM	SEARCH RADIUS (km)	MAX. NO POINTS	SD_E	r1	b1	r2	b2	STANDARDIZED RESIDUALS		
									Mean	SD	max
1987	Isotropic, nugget + spherical gamma(h) = 300000 + 330000 Sph_{50}(h)	25	8	791	0.46	0.83	0.35	0.51	0.03	1.12	-3.7
		"	4	783	0.47	0.79	0.39	0.53	0.06	1.08	-3.4
		"	2	789	0.43	0.60	0.44	0.51	0.11	1.02	-2.8
	Polygonal tessellation (estimate = nearest sample)	200	1	736	0.59	0.43	0.37	0.57	--	--	--
1988	Isotropic, nugget + linear gamma(h) = 100000 +13750(h)	50	12	926	0.37	0.52	0.25	0.44	-0.01	1.48	-3.8
		25	8	759	0.53	0.65	0.33	0.51	0.03	1.29	-3.7
		"	4	772	0.53	0.62	0.33	0.50	0.07	1.31	-3.5
		"	2	785	0.52	0.59	0.34	0.49	0.04	1.24	-3.4
	Polygonal tessellation (estimate = nearest sample)	200	1	1072	0.18	0.23	0.02	0.03	--	--	--
1989	Isotropic, nugget + linear gamma(h) = 750000 + 11818 h	25	8	1056	0.61	1.18	0.58	0.86	0.00	1.08	-4.5
		"	4	1040	0.63	1.13	0.60	0.81	0.04	1.02	-4.4
		"	2	981	0.63	0.98	0.68	0.77	0.03	0.89	-3.9
	Polygonal tessellation (estimate = nearest sample)	200	1	1249	0.51	0.51	0.56	0.52	--	--	--
1990	Isotropic, nugget + spherical gamma(h) = 1200000 + 700000 Sph_{20}(h)	50	12	1554	-0.05	-0.35	0.10	0.31	0.02	1.14	-3.6
		"	8	1579	-0.10	-0.63	0.08	0.22	0.04	1.15	-3.3
		25	8	1543	0.02	0.12	0.16	0.42	0.02	1.12	-3.1
		"	4	1598	0.09	0.40	0.12	0.27	-0.00	1.12	-3.5
		"	2	1694	0.12	0.39	0.10	0.16	-0.09	1.10	-3.6
	Isotropic, nugget gamma(h) = 1700000	50	12	1575	-0.17	-1.31	0.01	0.06	0.05	1.16	-3.6
		"	8	1640	-0.23	-1.43	-0.05	-0.14	0.07	1.18	-3.3
		25	8	1592	-0.08	-0.45	0.06	0.17	0.03	1.14	-3.2
		"	4	1662	-0.04	-0.21	0.02	0.05	0.01	1.14	-3.8
		"	2	1703	-0.07	-0.22	0.07	0.12	-0.09	1.07	-3.7
	Polygonal tessellation (estimate =nearest sample)	200	1	1875	0.27	0.25	0.19	0.20	--	--	--

Table 3. Estimated mass of shrimp (t) in the study region for 4 cutoff densities according to discrete summation of the kriging point estimates (kg/km^2) at the nodes of the interpolation grid (equation (6)), for the chosen kriging models (Table 1), the arithmetic mean and polygonal tessellation. The relative errors **SE = σ_D/total biomass** are computed from equations (7) and (9) for the kriging methods, and from equations (10) (11) and (9) for the polygonal tessellation. NR: non rigorously computable. FD: too few data (< 30 samples) to compute a meaningful variogram.

YEAR AND METHOD	ENVELOPE 4-13				ENVELOPE 1-3				TOTAL			
	mean X kg/km^2	area = km^2	mass t	SE %	mean X kg/km^2	area = km^2	mass t	SE %	mean X kg/km^2	area = km^2	mass t	SE %
1982												
Cutoff: ≥ 0 Kg/km^2												
Traditional variogram[1]	809.80	4700	3806	12.4	864.43	1325	1145	31.5	821.81	6025	4951	12.0
Arithmetic mean	769.28	4800	3693	NR	1168.00	1725	2015	NR	874.69	6525	5707	NR
Polygonal tessellation	795.26	4900	3897	15.8	680.61	1680	1143	47.9	765.99	6580	5040	16.4
Cutoff: ≥ 500 Kg/km^2												
Traditional variogram	1010.78	3225	3259	FD	1023.05	1075	1100	FD	1013.85	4300	4360	FD
Cutoff: ≥ 1000 Kg/km^2												
Traditional variogram	1363.65	1475	2011	FD	1192.72	675	805	FD	1309.99	2150	2816	FD
Cutoff: ≥ 1500 Kg/km^2												
Traditional variogram	1644.00	325	534	FD	1601.66	25	40	FD	1640.98	350	574	FD

---

[1] A fraction of the stratum could not be estimated because of absence of samples.

Table 3 (cont.)

YEAR AND METHOD	**ENVELOPE 4-13**				**ENVELOPE 1-3**				**TOTAL**			
	mean X	**area =**	**mass**	**SE**	**mean X**	**area =**	**mass**	**SE**	**mean X**	**area =**	**mass**	**SE**
	kg/km^2	**km^2**	**t**	**%**	**kg/km^2**	**km^2**	**t**	**%**	**kg/km^2**	**km^2**	**t**	**%**
1984												
Cutoff: ≥ 0 Kg/km^2												
Traditional variogram	660.72	4800	3171	9.3	968.31	1725	1670	11.4	742.04	6525	4842	7.1
Arithmetic mean	690.94	4800	3317	NR	975.77	1725	1683	NR	766.24	6525	5000	NR
Polygonal tessellation	614.12	4900	3009	11.4	973.46	1680	1635	15.6	705.87	6580	4645	9.2
Cutoff: ≥ 500 Kg/km^2												
Traditional variogram	677.06	4425	2996	8.7	968.31	1725	1670	8.8	754.06	6150	4637	5.7
Cutoff: ≥ 1000 Kg/km^2												
Traditional variogram	---	0	0	FD	1112.31	850	945	FD	1112.31	850	945	FD
Cutoff: ≥ 1500 Kg/km^2												
Traditional variogram	---	0	0	FD	---	0	0	FD	---	0	0	---
1985												
Cutoff: ≥ 0 Kg/km^2												
Traditional variogram	972.17	4800	4666	8.2	750.48	1725	1295	30.6	913.56	6525	5961	9.2
Arithmetic mean	1037.93	4800	4982	NR	593.50	1725	1024	NR	920.44	6525	6006	NR
Polygonal tessellation	1017.95	4900	4988	10.3	720.54	1680	1211	29.2	942.02	6580	6198	10.1
Cutoff: ≥ 500 Kg/km^2												
Traditional variogram	985.64	4675	4608	8.7	818.69	1400	1146	41.8	947.17	6075	5754	10.9
Cutoff: ≥ 1000 Kg/km^2												
Traditional variogram	1294.23	2050	2653	FD	1079.87	300	324	FD	1266.86	2350	2977	FD
Cutoff: ≥ 1500 Kg/km^2												
Traditional variogram	1578.33	450	710	FD	---	0	0	FD	1578.33	450	710	FD

Table 3 (cont.)

YEAR AND METHOD	ENVELOPE 4-13				ENVELOPE 1-3				TOTAL			
	mean X kg/km^2	area = km^2	mass t	SE %	mean X kg/km^2	area = km^2	mass t	SE %	mean X kg/km^2	area = km^2	mass t	SE %
1987												
Cutoff: ≥ 0 Kg/km^2												
Traditional variogram	1153.15	4800	5535	9.4	1189.52	1725	2052	15.3	1162.77	6525	7587	8.0
Arithmetic mean	1148.03	4800	5511	NR	1412.92	1725	2437	NR	1218.06	6525	7948	NR
Polygonal tessellation	1068.96	4900	5238	12.7	1213.86	1680	2039	14.6	1105.96	6580	7277	10.0
Cutoff: ≥ 500 Kg/km^2												
Traditional variogram	1210.80	4450	5388	8.9	1189.52	1725	2084	14.7	1204.86	6175	7440	7.6
Cutoff: ≥ 1000 Kg/km^2												
Traditional variogram	1545.95	2500	3865	FD	1365.40	1150	1570	FD	1489.06	3650	5435	FD
Cutoff: ≥ 1500 Kg/km^2												
Traditional variogram	1861.66	1350	2513	FD	1688.91	425	718	FD	1820.30	1775	3231	FD
1988												
Cutoff: ≥ 0 Kg/km^2												
Traditional variogram	781.03	4800	3749	10.4	1906.02	1725	3288	7.8	1078.44	6525	7037	6.6
Arithmetic mean	697.02	4800	3346	NR	2048.62	1725	3534	NR	1054.34	6525	6880	NR
Polygonal tessellation	766.13	4900	3754	16.4	1991.20	1680	3345	10.0	1078.91	6580	7099	10.1
Cutoff: ≥ 500 Kg/km^2												
Traditional variogram	853.86	4000	3415	11.0	1928.83	1700	3279	7.9	1174.47	5700	6694	6.8
Cutoff: ≥ 1000 Kg/km^2												
Traditional variogram	1448.08	950	1376	FD	2027.17	1575	3193	FD	1809.29	2525	4568	FD
Cutoff: ≥ 1500 Kg/km^2												
Traditional variogram	1806.82	375	678	FD	2095.91	1450	3039	FD	2036.51	1825	3717	FD

Table 3 (cont.)

YEAR AND METHOD	**ENVELOPE 4-13**				**ENVELOPE 1-3**				**TOTAL**			
	mean X kg/km^2	**area = km^2**	**mass t**	**SE %**	**mean X kg/km^2**	**area = km^2**	**mass t**	**SE %**	**mean X kg/km^2**	**area = km^2**	**mass t**	**SE %**
1989												
Cutoff: ≥ 0 Kg/km^2												
Traditional variogram	981.05	4800	4709	13.0	2688.79	1725	4638	6.3	1432.52	6525	9347	7.9
Arithmetic mean	1098.76	4800	5274	NR	2517.25	1725	4342	NR	1473.76	6525	9616	NR
Polygonal tessellation	967.92	4900	4743	11.8	2596.83	1680	4363	11.1	1383.81	6580	9105	7.5
Cutoff: ≥ 500 Kg/km^2												
Traditional variogram	1155.60	3775	4362	14.5	2688.79	1725	4638	7.3	1636.46	5500	9001	8.0
Cutoff: ≥ 1000 Kg/km^2												
Traditional variogram	1811.61	1425	2582	12.4	2785.88	1650	4597	7.5	2334.39	3075	7178	6.5
Cutoff: ≥ 1500 Kg/km^2												
Traditional variogram	2097.77	925	1940	11.2	3054.23	1425	4352	5.5	2677.75	2350	6293	5.1
1990												
Cutoff: ≥ 0 Kg/km^2												
Traditional variogram	1344.79	4800	6455	13.0	2293.15	1725	3956	14.7	1595.51	6525	10411	9.8
Arithmetic mean	1353.63	4800	6497	NR	2166.64	1725	3737	NR	1568.56	6525	10235	NR
Polygonal tessellation	1351.52	4900	6622	14.2	2475.81	1680	4159	24.8	1638.57	6580	10782	12.9
Cutoff: ≥ 500 Kg/km^2												
Traditional variogram	1344.79	4800	6455	13.9	2349.49	1675	3935	17.2	1604.69	6475	10390	10.8
Cutoff: ≥ 1000 Kg/km^2												
Traditional variogram	1502.00	3750	5633	14.3	2405.43	1625	3909	16.8	1775.13	5375	9541	10.9
Cutoff: ≥ 1500 Kg/km^2												
Traditional variogram	1973.91	1325	2615	FD	2405.43	1625	3909	FD	2003.80	2128	4264	FD

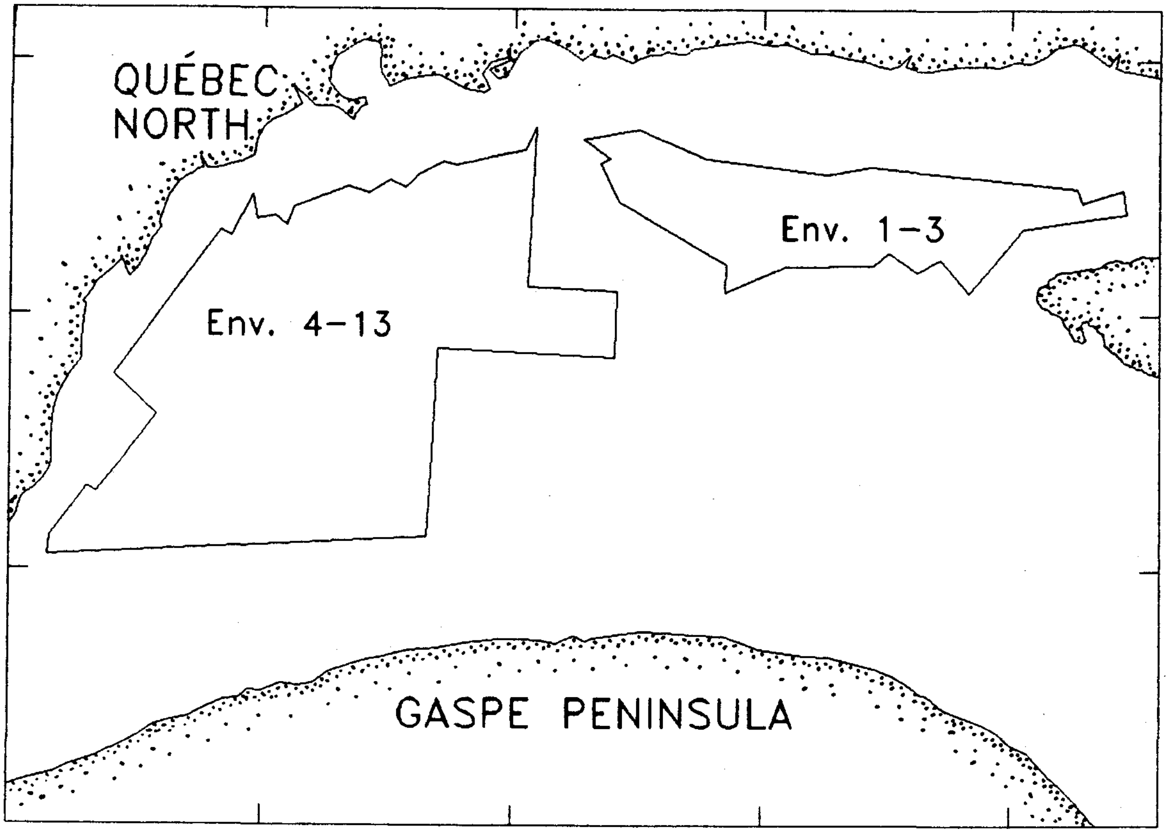

Figure 1. Map of the western Gulf of St.Lawrence with the east (Env. 1-3) and west (Env. 4-13) envelopes of biomass estimation of the Sept-Iles northern shrimp fishing ground. Tic spacing on the borders are 50 km.

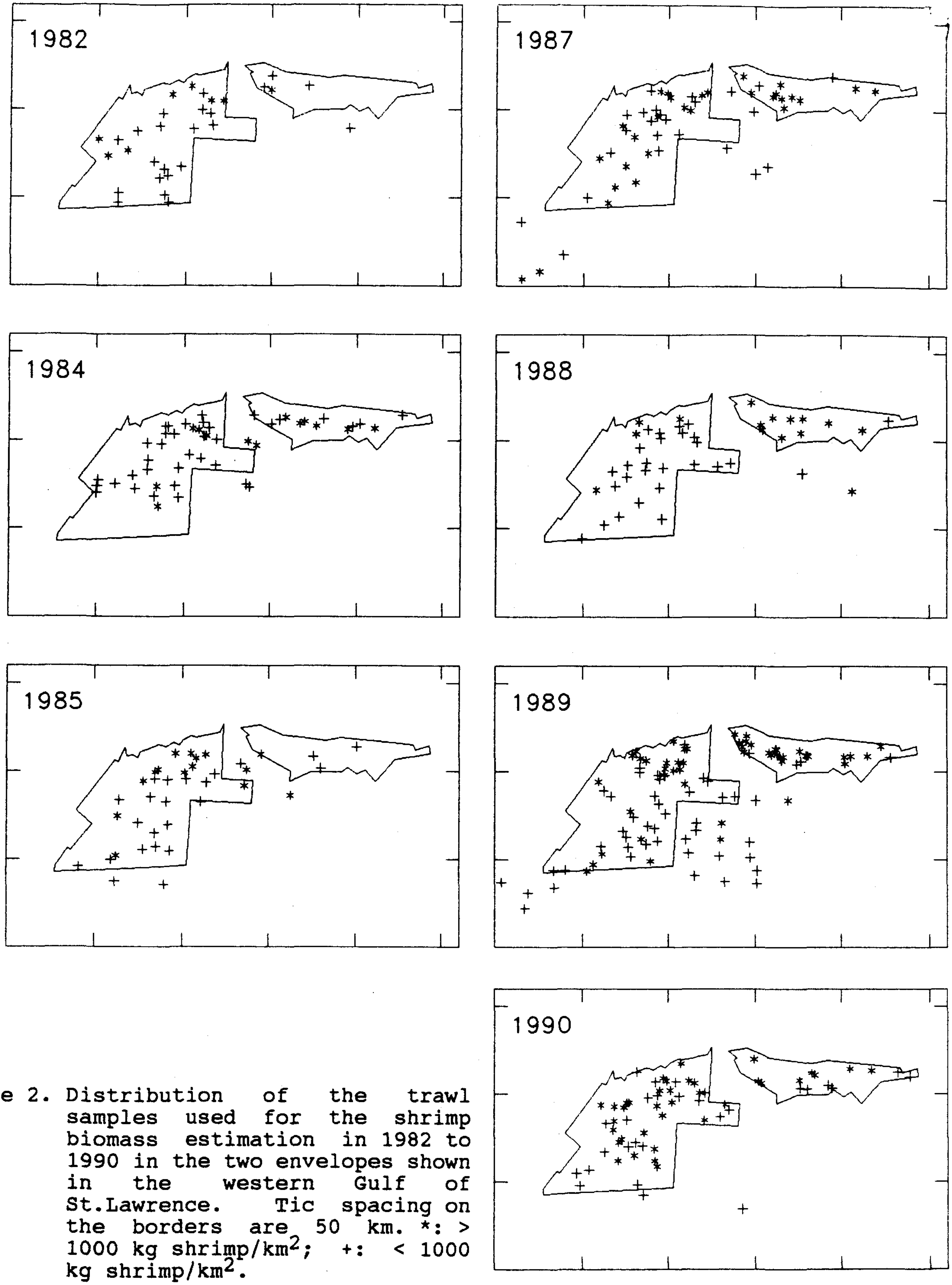

Figure 2. Distribution of the trawl samples used for the shrimp biomass estimation in 1982 to 1990 in the two envelopes shown in the western Gulf of St.Lawrence. Tic spacing on the borders are 50 km. *: > 1000 kg shrimp/km^2; +: < 1000 kg shrimp/km^2.

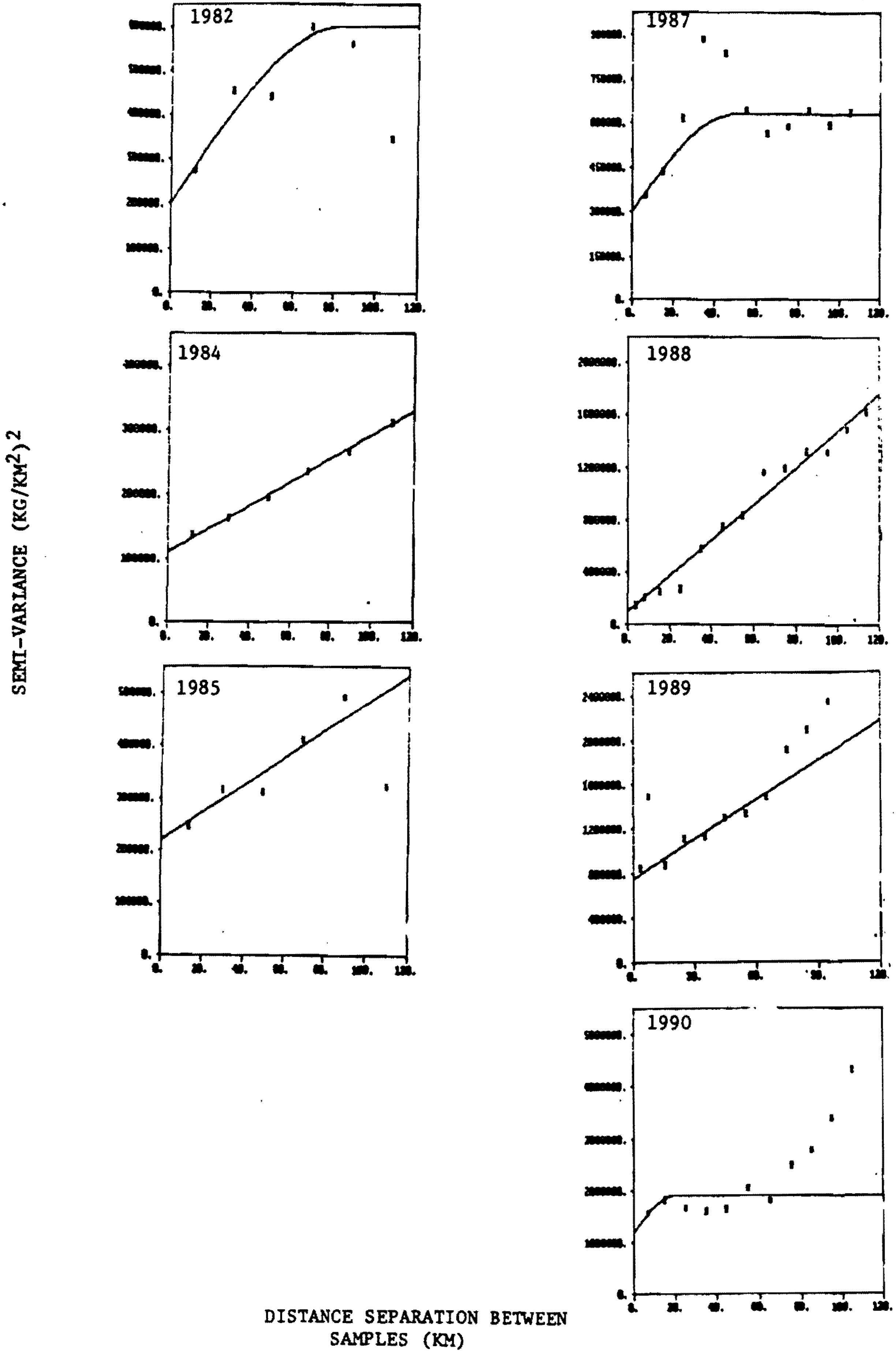

Figure 3. Experimental omnidirectional semi-variogram computed from the shrimp biomass samples shown in Fig. 2. The variogram functions fitted are given in Table 2 (underlined). Note the different scales of semi-variance.

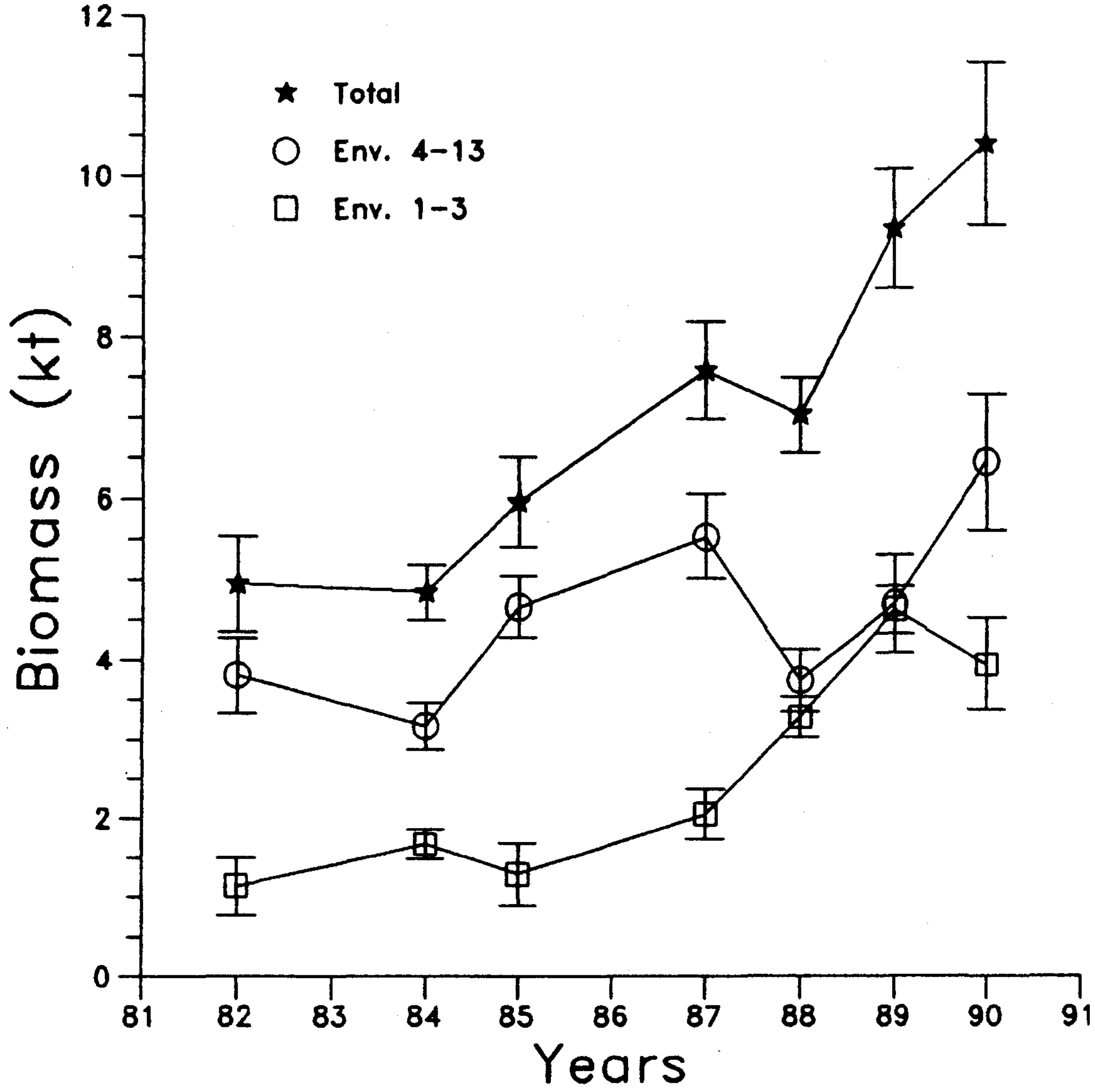

Figure 4. Time series of the kriged **global** estimates of the northern shrimp biomass in the study area in the western Gulf of St.Lawrence from 1982 to 1990, for the two envelopes shown in Fig. 1, taken separately or combined. The bars represent 2 SE of the estimates. **N.B.** The 1982 estimates are underestimated because they correspond to only 77%, 98% and 92% of the areas for the envelope 1-3, the envelope 4-13 and the total surveyed area, respectively.

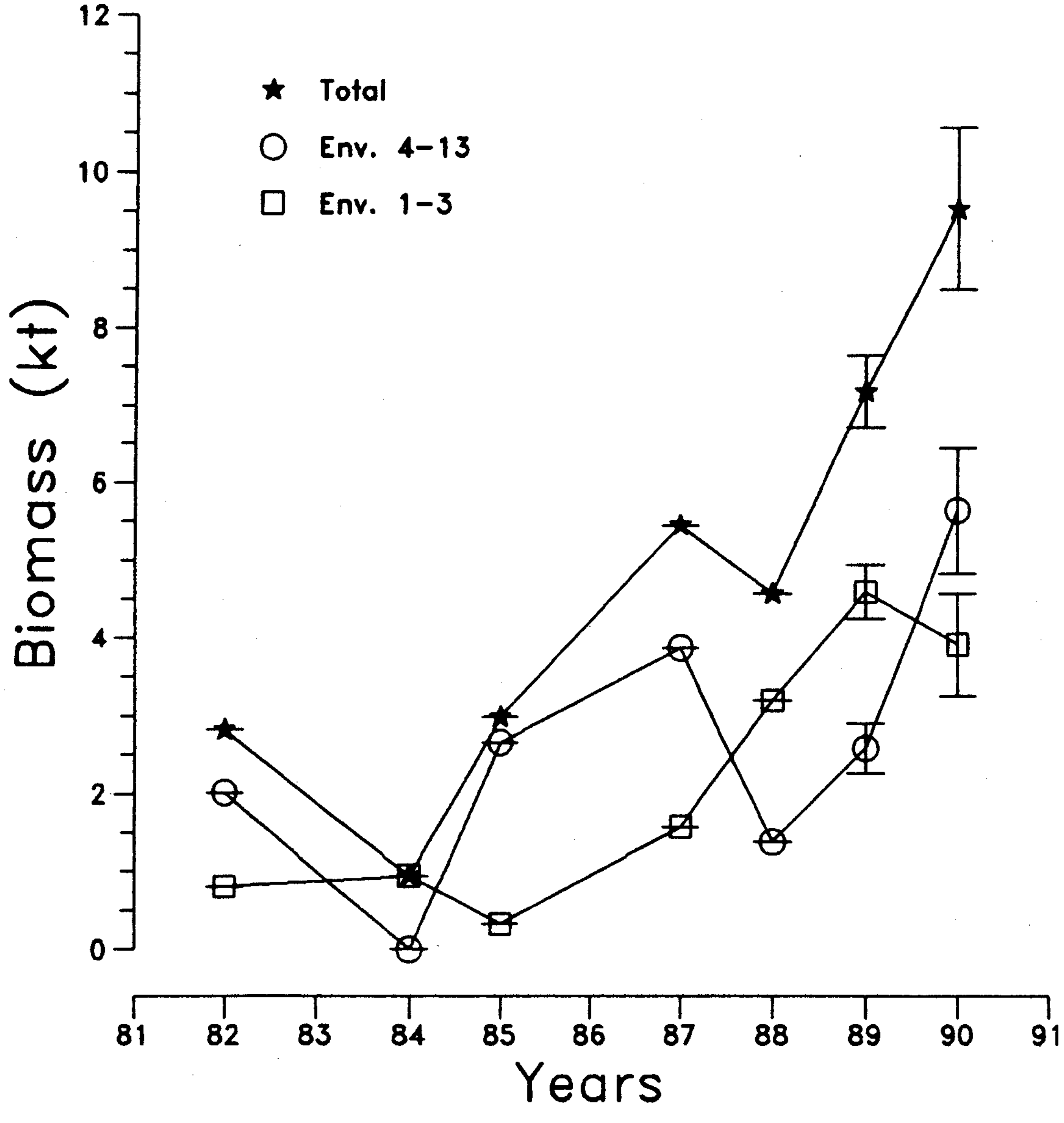

Figure 5. Time series of the kriged **partial** estimates (see text) of the northern shrimp biomass for the cutoff density of 1 t/km^2 in the study area in the western Gulf of St.Lawrence from 1982 to 1990, for the two envelopes shown in Fig. 1, taken separately or combined. The bars represent 2 SE of the estimates. **N.B.** The 1982 estimates are underestimated because they correspond to only 77%, 98% and 92% of the areas for the envelope 1-3, the envelope 4-13 and the total surveyed area, respectively.

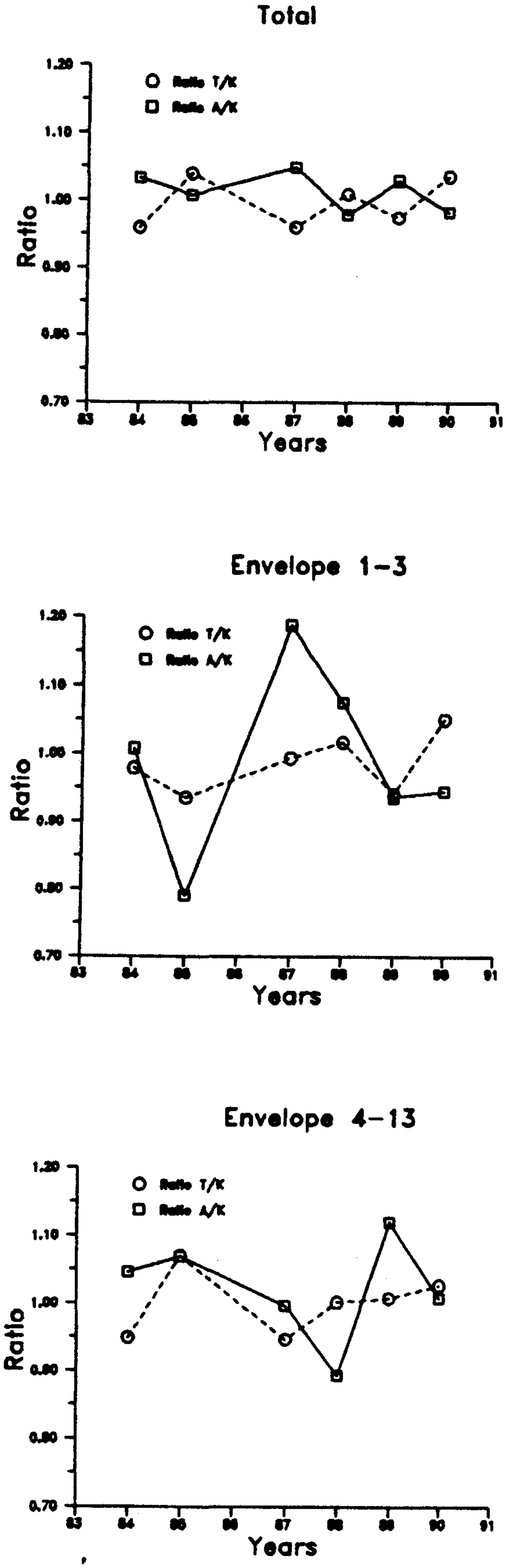

Figure 6. Time series of the ratio of the global estimate of the northern shrimp biomass in the western Gulf of St.Lawrence from polygonal tessellation (T) and from the arithmetic mean (A) versus the kriged estimate (K) for 1984 to 1990, for the two envelopes shown in Fig. 1, taken separately or combined.